

RESEARCH

## *Afzelia quanzensis* bark extract for green synthesis of silver nanoparticles and study of their antibacterial activity

Mambo Moyo<sup>1</sup> · Makore Gomba<sup>1</sup> · Tichaona Nharingo<sup>1</sup>

Received: 14 September 2014 / Accepted: 10 September 2015

© The Author(s) 2015. This article is published with open access at Springerlink.com

**Abstract** In the present study, *Afzelia quanzensis* bark extract was tested for the biosynthesis of silver nanoparticles (AgNPs). Based on UV–Vis spectrum analysis, the characteristic absorption band was observed at 427 nm. Furthermore, the size and shape of the nanoparticles ranged from 10 to 80 nm and were spherical in shape as observed through SEM analysis. In addition, the X-ray diffraction analysis showed that the silver nanoparticles are crystalline in nature and have a face-centred cubic structure. Based on FTIR analysis, the presence of phytochemical functional groups such as carboxyl (–C=O) and amine (N–H) in *Afzelia quanzensis* bark extract further confirmed the responsible reducing agents for nanoparticles formation. Interestingly, the synthesized silver nanoparticles at 50 mg/L concentration showed significant antibacterial activity against *Escherichia coli* and *Staphylococcus aureus*.

**Keywords** Biological synthesis · Silver nanoparticles · Bark extract · Antibacterial activity

### Introduction

At present, nanotechnology is a rapidly developing field of importance since it deals with the synthesis and stabilization of different metal nanoparticles. Among the particles, silver nanoparticles (AgNPs) have become the focus of intensive research due to several important applications

such as their use in bio-labelling, sensors, drug delivery system, antimicrobial agents and filters [1, 2]. The synthesized silver nanoparticles exhibit new or improved properties depending upon their size, morphology and distribution [3]. The production of pure and well-defined metal-based nanoparticles by chemical reduction [4], thermal treatment, irradiation [5] and laser ablation [6] have been reported. On one hand, organic solvents, toxic reducing agents, high-pressure and high-temperature conversion which are potentially dangerous to the environment are used [7]. Hence, a pressing need to shift from physical and chemical synthesis to ‘green’ chemistry and bioprocesses is of major interest.

In the last decade, the biosynthesis of nanoparticles has received increasing attention due to the growing need to develop environmentally benign technologies in material synthesis [8, 9]. Biological routes for the synthesis of metal nanoparticles by exploiting bacteria [10, 11], marine fungus *Penicillium fellutanum* [1], fungus *Aspergillus foetidus* [12], yeast [13, 14], enzymes [15] have been reported. However, one of the major drawbacks in using microbes for nanoparticle synthesis is the elaborate process of maintaining microbial cultures. The use of plant extracts for the synthesis of nanoparticles have gained momentum in recent years and could be advantageous over other environmentally benign biological processes by eliminating the elaborate process of maintaining cell cultures, being simply, eco-friendly and this could be an exciting possibility that is relatively unexplored and under exploited [16]. Green silver nanoparticles synthesis using various natural products like *Magnolia kobus* [17], *Acacia leucophloea* extract [18], *Zizyphus xylopyrus* bark extract [19], *aloevera* plant extract [20, 21], *Cinnamon zeylanicum* bark extract [22], *Curcuma longa* tuber powder [23] and *Jatropha curcas* [9] have been reported. However, the

✉ Mambo Moyo  
moyom@msu.ac.zw

<sup>1</sup> Department of Chemical Technology, Faculty of Science, Midlands State University, P. Bag 9055, Senga, Gweru, Zimbabwe

potential of other plants as sources of biomaterial for the synthesis of new nanoparticles are yet to be entirely explored.

It has been reported that plants contain different phytochemical products [24] which are able to breakdown the silver nitrate, a complex hazardous chemical into  $\text{Ag}^+$  and  $\text{NO}_3^-$  ions. In the process, the toxic  $\text{Ag}^+$  ions are further reduced to the nontoxic ( $\text{Ag}^0$ ) metallic nanoparticles through the use of different functional groups on the surface of the extract [25]. In the present study, we selected *Azelia quanzensis*, Pod mahogany (English), Mujarakamba (Shona name in Zimbabwe) bark as a biomaterial for supplying the different phytochemicals required for the synthesis of silver nanoparticles and the mechanism involved in the synthesis is illustrated in Fig. 1. The plant is economic and abundantly available in Zimbabwe. It is a medium-sized to large deciduous tree and has a bark which is greyish-brown, flaking and leaving pale patches [26]. It produces fruits which consist of a large flattened pod, thickly woody, 10–17 cm, and splitting to reveal large, shiny black seeds with a bright red aril. In medicine, roots are used to treat gonorrhoea, chest pains, kidney problems, bilharzia, eye problems and snakebites, and a small piece of bark is applied to an aching tooth. The plant can be categorized as:

Taxonomy

Kingdom: Plantae

Division: Tracheophyta

Subdivision: Spermatophytina

Class: Magnoliopsida

Order: Fabales

Family: Fabaceae

Genus: *Azelia* Sm.—mahogany

Species: *Azelia quanzensis* Welw.—pod mahogany

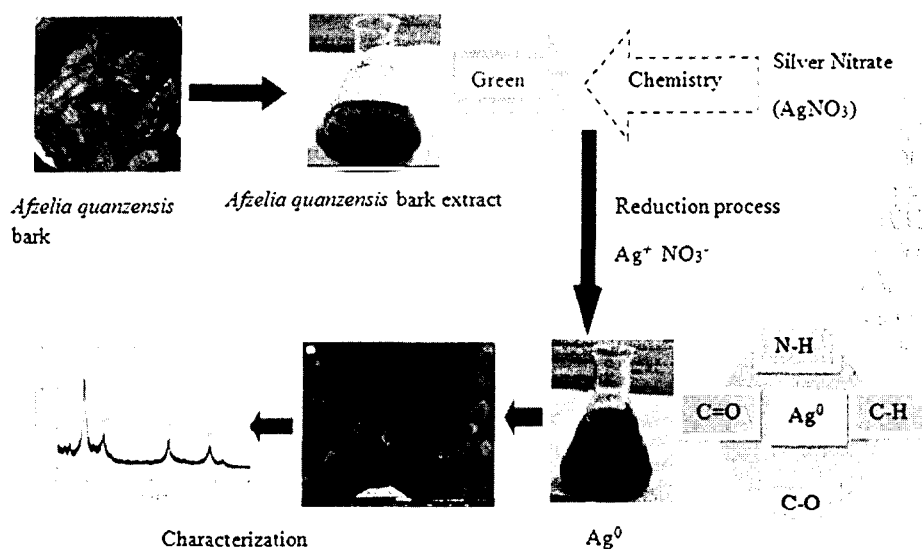
In the present study, we used plant bark extracts for synthesis of silver nanoparticles by monitoring their conversion using UV–visible spectroscopy. We also investigated the effects of reaction conditions such as temperature, pH, quantities of bark extract and  $\text{AgNO}_3$  concentration on the synthesis rate. The silver nanoparticles were further characterized by X-ray diffraction (XRD), scanning electron microscopy (SEM), energy dispersive X-ray (EDX) spectrometer, and Fourier transform infrared spectroscopy (FTIR). Furthermore, the antibacterial activity of the silver nanoparticles on a strain of *Escherichia coli* and *Staphylococcus aureus* was qualitatively evaluated by the zone inhibition method.

## Materials and methods

### Preparation of *Azelia quanzensis* bark powder and extract

The bark was obtained from *Azelia quanzensis* tree in Chivi rural district area, Zimbabwe. The bark was washed to remove any impurities and dried under sunlight for a week to completely remove the moisture. The bark was cut into small pieces, powdered in a mixer and then sieved using a 20-mesh sieve to get uniform size range. The sieved powder was used for all further studies. For the production of an extract, 50 g of powdered bark was added to a 500-mL Erlenmeyer flask containing 200 mL deionized water and then boiled for 15 min. After cooling, the mixture was filtered through Whatman filter paper no. 1 and the extract was kept at 4 °C prior to silver nanoparticles synthesis.

**Fig. 1** Mechanism involved in the synthesis of silver nanoparticles using *Azelia quanzensis* extract



130	<b>Synthesis of silver nanoparticles</b>		
131	Silver nitrate (AgNO <sub>3</sub> ) analytical grade used as a precursor	4000 cm <sup>-1</sup> . FTIR measurements were made to identify the	173
132	was purchased from Sigma-Aldrich (Pretoria, South	possible biomolecules responsible for capping and efficient	174
133	Africa). For the AgNPs synthesis, 5 mL bark extract were	stabilization of the synthesized silver nanoparticles.	175
134	added to 50 mL of 1 mM aqueous AgNO <sub>3</sub> solution in a		
135	250-mL Erlenmeyer flask. The flask was then incubated in	<b>Study for the influence of different parameters</b>	176
136	a rotary shaker at 160 rpm in the dark. The reduction of	Influence of different temperatures (30, 40, 50, 60, 70, 80,	177
137	silver ions was routinely monitored visually for colour	90 °C), pH values (3, 5, 7, 8, 11), bark extract amounts (2,	178
138	change at regular intervals. Thereafter, the silver	4, 6, 8, 10, 12, 14 mL), substrate concentrations (1, 3, 5, 7,	179
139	nanoparticle solution thus obtained was purified by repeated	9, 11, 13 mM AgNO <sub>3</sub> ) and incubation periods (20, 40, 60,	180
140	centrifugation at 500 rpm for 20 min followed by re-	80, 100, 120, 140 min) were investigated by varying the	181
141	dispersion of the pellet of silver nanoparticles into a 10 mL	parameters one at a time. A sample of 1 mL was with-	182
142	of deionized water. After freeze drying, lyophilization	drawn at different time intervals and the absorbance was	183
143	process was performed on the purified silver nanoparticles	measured at 427 nm.	184
144	to obtain the powdered form which was stored in brown		
145	bottles prior to physical characterization and antibacterial	<b>Measuring concentration of AgNPs using</b>	185
146	activity.	<b>inductively coupled plasma optical emission</b>	186
		<b>spectrophotometer (ICP-OES)</b>	187
147	<b>Characterization</b>		
148	<i>UV-Vis spectrophotometer analysis</i>	The original concentration (80 mg/L) of the <i>Azelia</i>	188
149	The preliminary reduction of synthesized silver nanopar-	<i>quanzensis</i> bark extract mediated AgNPs was measured	189
150	ticles was monitored using UV-visible spectrophotometer	using ICP-OES. Then, by diluting this solution, samples of	190
151	(Shimadzu UV-1601, Japan) by scanning the absorbance	different concentrations (10, 25, 50 mg/L) were used to	191
152	spectra in the range of 300–600 nm. All sample solutions	investigate the concentration dependence of the antibacte-	192
153	were diluted using a ratio of 1:10.	rial effect of Ag nanoparticles.	193
154	<i>Electron microscopic study</i>	<b>Evaluation of antibacterial activity of synthesized</b>	194
155	SEM analysis of the synthesized silver nanoparticles was	<b>silver nanoparticles</b>	195
156	done using a Hitachi S-4500 SEM machine (Japan). A thin	The synthesized silver nanoparticles were tested for their	196
157	layer of gold was used to coat the samples through vacuum	antibacterial activity by using the disk diffusion method.	197
158	evaporation so that the nanoparticles conducts evenly and	The cultures of <i>Staphylococcus aureus</i> (ATCC-25923) and	198
159	provides a homogeneous surface for analysis and imaging	<i>Escherichia coli</i> (ATCC-39403) were obtained from	199
160	on an aluminium slab. The elemental analysis was per-	American Type Culture Collection Center, USA. <i>S. aureus</i>	200
161	formed using EDX (JEOL-JSM-5800LV, Tokyo, Japan)	and <i>E. coli</i> were grown on Mueller–Hinton agar medium.	201
162	which is an attachment to the SEM. The sample powder of	The disk diffusion was performed by placing different	202
163	AgNPs was compressed to form tablets before analysis	types of disks including bark extract (50 µL), synthesized	203
164	with EDX spectrum.	silver nanoparticles (50 µL/10, 25, 50 mg/L), standard	204
165	<i>XRD analysis</i>	antibiotic (erythromycin 50 µL) and synthesized silver	205
166	The dried synthesized silver nanoparticles were analysed	nanoparticles with standard antibiotic on the surface of the	206
167	using an X-ray diffractometer (D8 Bruker, Germany) with	agar in plates and incubated for 24 h at 37 °C. The zones of	207
168	Cu K <sub>α</sub> radiation in the range of 30° ≤ 2θ ≤ 90° at 40 kV	inhibition were measured by the Hi-Media scale.	208
169	and 40 mA.		
170	<i>FTIR analysis</i>	<b>Results and discussion</b>	209
171	FTIR (PerkinElmer, US) spectra were obtained at room	<b>Visual analysis</b>	210
172	temperature in the spectral range between 480 and	<i>Azelia quanzensis</i> bark extract when incubated with	211
		AgNO <sub>3</sub> solution under dark conditions changed its colour	212
		from colourless to light reddish and finally to reddish	213
		brown. The colour of the filtrate changed to intense brown	214
		after 120 min of incubation (Fig. 2b, c). The control	215

**Fig. 2** Optical photograph of 1 mM AgNO<sub>3</sub> solution (a) filtrate with silver ions at the beginning of reaction (b) and after 120 min of reaction (c)

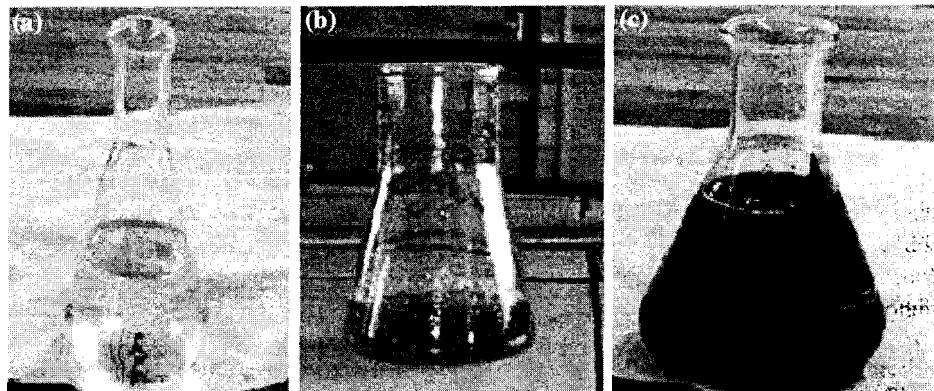
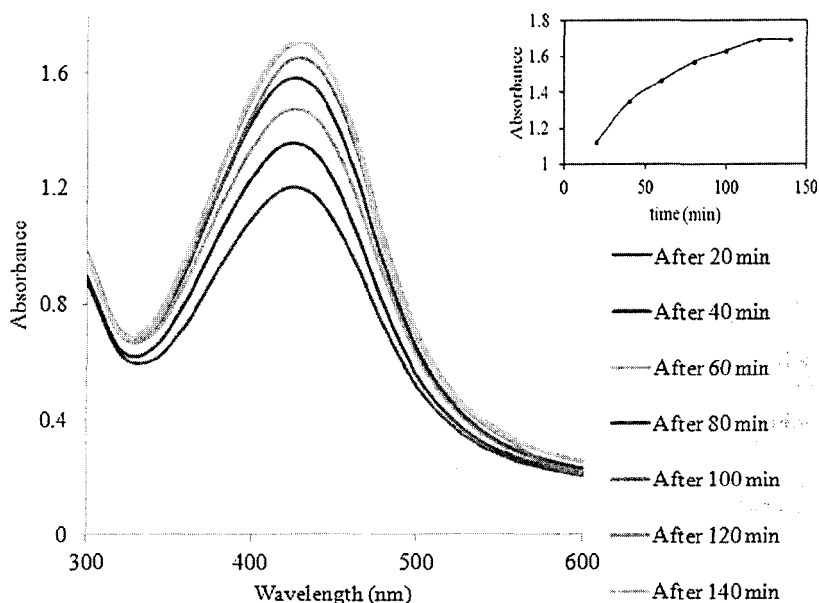
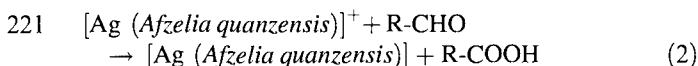
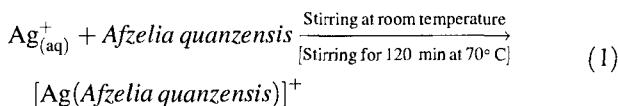


**Fig. 3** The UV-visible absorption spectra of synthesized AgNPs. The inset shows the change in SPR as a function of time



216 AgNO<sub>3</sub> solution (without *Afzelia quanzensis* bark extract) 229  
 217 showed no change in colour (Fig. 2a). The possible 230  
 218 chemical reactions involved in the preparation of the 231  
 219 AgNPs can be represented as: 232



## 223 UV-Vis spectra analysis 224

225 The development of metal silver nanoparticles in aqueous 226  
 227 solution was described by UV-Vis spectroscopy. The 228  
 228 absorption spectra of AgNPs formed at different durations 229  
 are shown in (Fig. 3).

From Fig. 3, it can be observed that the plasmon band 229  
 was symmetric, indicating that the solution does not have 230  
 much aggregated particles [27]. The evolution of an 231  
 absorption spectra for the AgNPs shows an increasingly 232  
 sharp absorbance at 427 nm with increase in time, which 233  
 steadily increased in intensity as a function of reaction 234  
 time without showing any shift of the maximum wavelength [2]. 235  
 This phenomenon may be linked to polarization of the free 236  
 conduction electrons with respect to the much heavier ionic 237  
 core of AgNPs, resulting in electron dipolar oscillation 238  
 after exposure of AgNPs to light [12]. For quality assurance 239  
 and comparison, AgNO<sub>3</sub> solution in deionized water 240  
 showed no absorption peak at the same wavelength range 241  
 (data not shown). In the present bark extract/Ag investigation, 242  
 the reaction mixtures showed a single SPR band 243  
 revealing the spherical shape of AgNPs which is in good 244  
 agreement to the Mie's theory [28]. Consequently, this 245

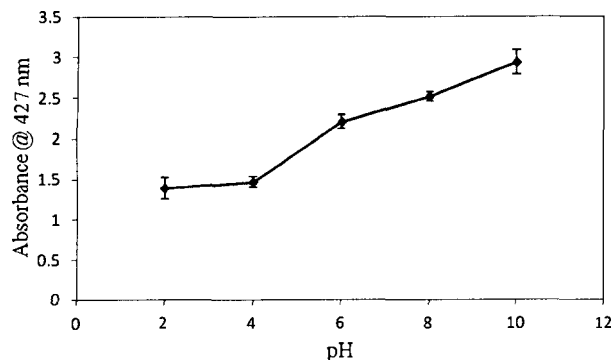


Fig. 4 Effect of different pH on nanoparticle production (error bar  $\pm$ SD and  $n = 3$ )

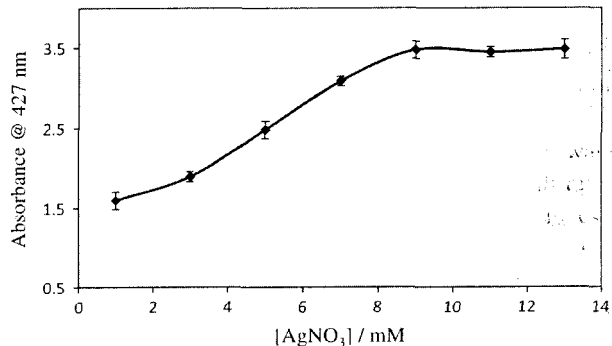


Fig. 5 Effect of AgNO<sub>3</sub> concentration (error bar  $\pm$ SD and  $n = 3$ )

246 validates the application of *Afzelia quanzenis* bark extract  
247 as a precursor for AgNPs synthesis.

#### 248 Study for the influence of different parameters

249 The biosynthesis of AgNPs is affected by a variety of  
250 factors (substrate concentration, electron donor, incubation  
251 time, pH, temperature, buffer strength, etc.) which control  
252 the shape and size as well as achieving the monodispersity  
253 in solution phase. In this study, the effects of pH, AgNO<sub>3</sub>  
254 concentrations, different quantities of bark extract, and  
255 different temperatures were investigated.

#### 256 Effect of pH

257 The size and morphology of nanoparticles are mainly  
258 affected by the pH of solution [29–31]. As shown by UV–  
259 Vis spectroscopy (Fig. 4), when the pH of the reaction  
260 mixture was increased, an increase in absorbance was  
261 observed. This might be due to the increase in production  
262 of colloidal silver nanoparticles and reduction rate. Visual  
263 observation showed the amount of nanoparticles to be pH  
264 value dependent. The reaction mixture colouring acceler-  
265 ated when the pH was increased. At acidic pH, large-sized  
266 silver nanoparticles were observed, whilst at higher pH  
267 highly dispersed, small-sized nanoparticles were formed.  
268 The results are in agreement with those reported in litera-  
269 ture [32–34]. Control experiments (AgNO<sub>3</sub> solution incu-  
270 bated at different alkaline pH 8, 9, 10) showed no synthesis  
271 of nanoparticles.

#### 272 Effect of AgNO<sub>3</sub> concentration

273 The concentration of AgNO<sub>3</sub> which might be converted to  
274 a final product is one of the important measures required to  
275 make the reaction more economical and efficient [31]. The  
276 effect of AgNO<sub>3</sub> concentration on synthesis of AgNPs is  
277 shown in Fig. 5.

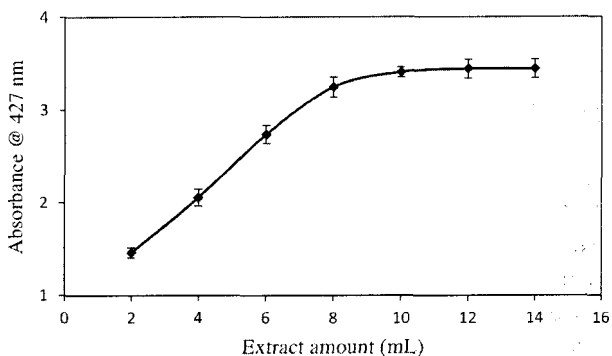
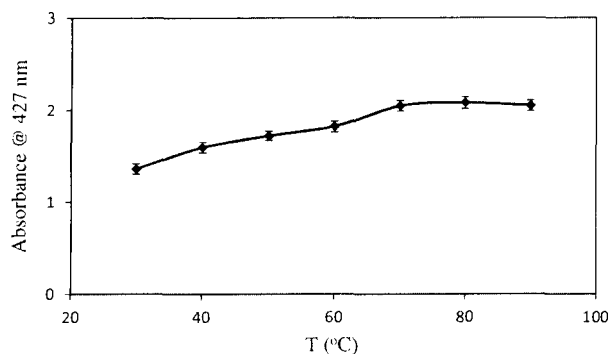


Fig. 6 Effect of different quantities of *Afzelia quanzenis* bark extract (error bar  $\pm$ SD and  $n = 3$ )

278 There was an increase in synthesis of AgNPs with  
279 respect to Ag<sup>+</sup> ion concentration in the range 1–9 mM.  
280 However, the absorbance was found to decrease at con-  
281 centrations greater than 9 mM. Comparable results were  
282 obtained for the synthesis AgNPs using *Pinus eldarica* bark  
283 extract [31]. Consequently, 9 mM was used for further  
284 studies.

#### 285 Effect of different quantities of *Afzelia quanzenis* bark 286 extract

287 The production of AgNPs was monitored as a function of  
288 different amounts of *Afzelia quanzenis* bark extract  
289 amount. Figure 6 shows the effect of extract amount on  
290 AgNPs production. The increase in the extract amount  
291 from 2 to 10 mL caused a considerable increase in peak  
292 absorbance in UV–Vis spectrum. The increase in the  
293 amount of soluble phytochemical reducing agents in the  
294 extract would mean more Ag<sup>+</sup> ion reduction, and subse-  
295 quently more nanoparticle production. Furthermore, a  
296 decrease in amount of Ag nanoparticles was observed due  
297 to an increase in extract amount above 10 mL.



**Fig. 7** Effect of reaction temperature (error bar  $\pm$ SD; and  $n = 3$ )

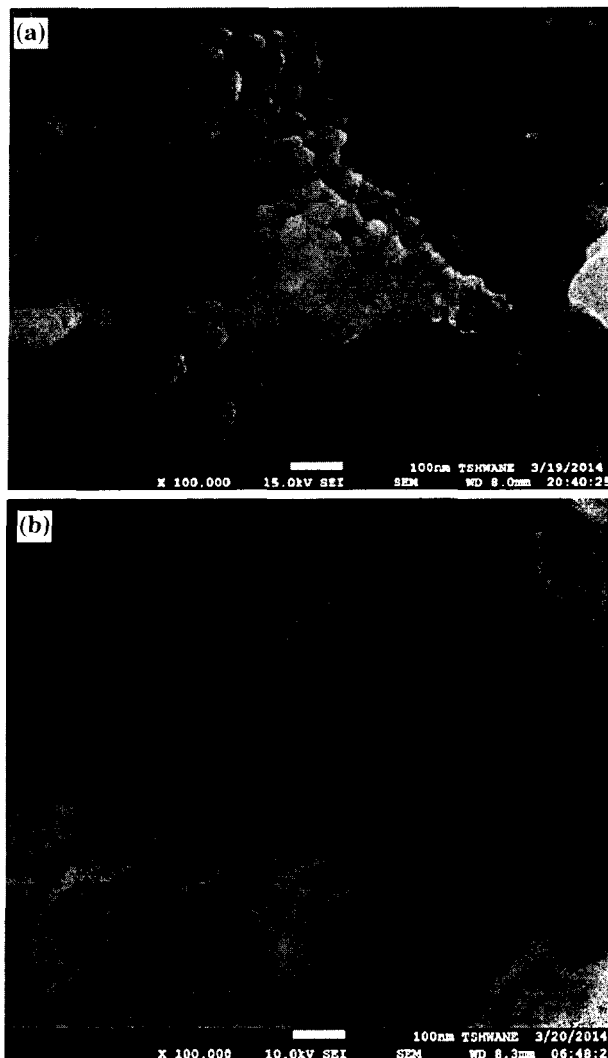


**Fig. 8** Scanning electron microscopic observation of a silver nitrate and b synthesized

clearly illustrates that the silver nanoparticles formed in this present synthesis are crystalline in nature. There were no other corresponding peaks observed from the XRD pattern which showed that the formed AgNPs have a high purity. Previous studies have also reported the crystalline nature of biosynthesized AgNPs using different plant extracts [3, 9, 22, 23, 36]. The average crystalline size of silver nanoparticles synthesized using *Azela quanzensis* bark extract can be calculated using the Scherrer equation [25]:

$$D = \frac{K\lambda}{\beta \cos\theta} \quad (3)$$

where  $D$  is the crystallite size of AgNPs,  $\lambda$  is the wavelength of the X-ray source (0.1541 nm),  $\beta$  is the full width at half maximum of the diffraction peak,  $K$  is the Scherrer

## 298 Effect of temperature

299 The role of temperature on the reaction rate from 30 to  
300 70 °C was investigated. An increase in absorbance was  
301 noted as the temperature increased (Fig. 7). The enhanced  
302 rate of synthesis of AgNPs might be due to the reaction  
303 temperature increasing the kinetic energy of the reacting  
304 molecules thus more  $\text{Ag}^+$  ions were in collision with the  
305 reducing molecules of the extract. The maximal synthesis  
306 of AgNPs was achieved at 70 °C.

## 307 Characterization

### 308 Electron microscopic study

309 The SEM images of the  $\text{AgNO}_3$  (Fig. 8a) and synthesized  
310 silver nanoparticles (Fig. 8b) were clearly noticeable. The  
311 size of the silver nitrate particles used as control in this  
312 study was greater than 1 000 nm size (Fig. 8a); whereas,  
313 the synthesized silver nanoparticles measured 10–80 nm in  
314 size (Fig. 8b). Similar to our study, the same pattern of  
315 silver nanoparticles were also reported [24]. The EDAX  
316 spectroscopy results confirmed the significant presence of  
317 61.66 % silver, 30.47 % carbon and oxygen 7.87 %  
318 (Fig. 9). Metallic silver nanocrystals generally show a  
319 typical optical absorption peak approximately at 3 keV due  
320 to surface plasmon resonance [35]. The weak signals at  
321 0.25 and 0.50 keV were are for carbon and oxygen,  
322 respectively, which might arise from the functional com-  
323 pounds present in the aqueous extract.

### 324 XRD: purity and crystalline nature of AgNPs

325 The phase of the vacuum dried nanoparticles was investi-  
326 gated by XRD and corresponding patterns are shown in  
327 Fig. 10. However, silver nanoparticles have shown clear  
328 peaks of cubic phases (JCPDS No. 03-0921) at 38.1 (111),  
329 42.9 (200), 65.5 (220) and 77.9 (311). XRD pattern thus

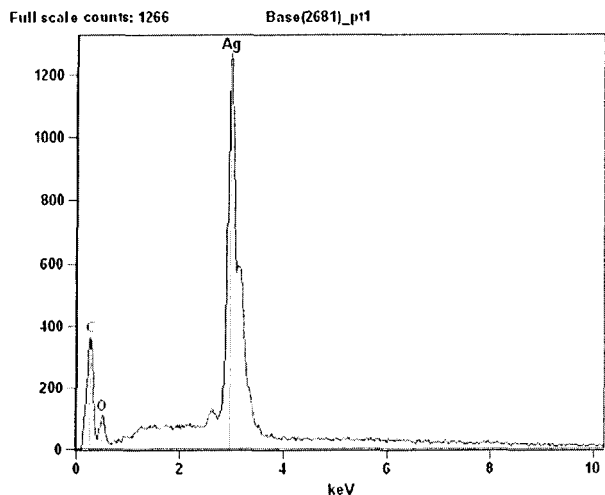


Fig. 9 The EDX spectrum for AgNPs

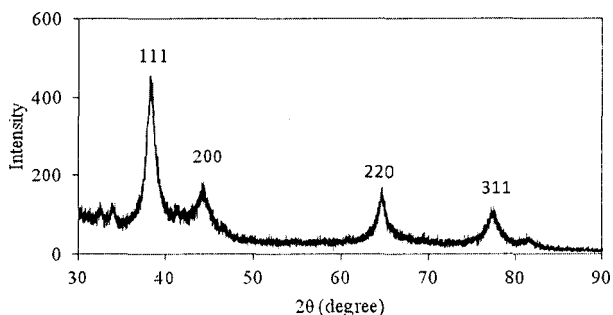


Fig. 10 XRD spectra of AgNPs

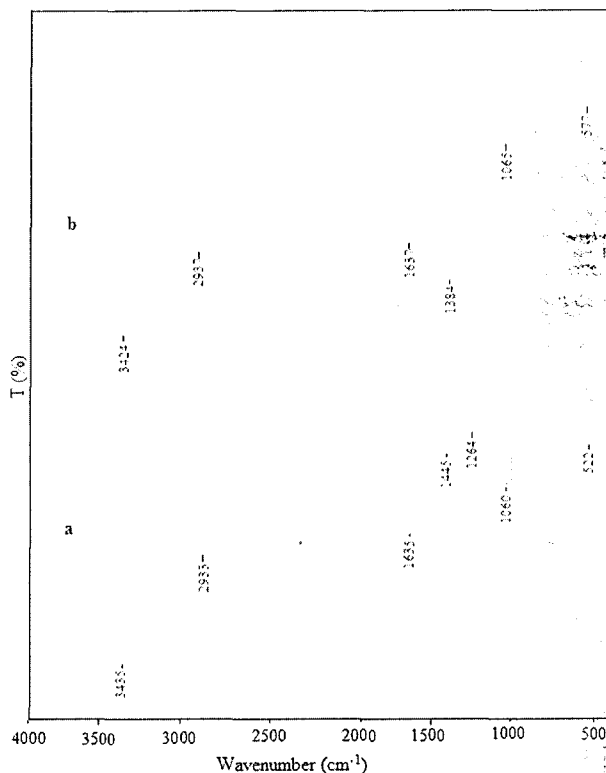


Fig. 11 FTIR spectra of *Afzelia quanzensis* extract (a) and synthesized AgNPs (b)

and alkyl group decreased in intensity, and shifted to 2937  $\text{cm}^{-1}$ . The disappearance of the peaks at 1445 and 1264  $\text{cm}^{-1}$  and formation of new intense peak at 1384  $\text{cm}^{-1}$ , signify the involvement of the secondary amines in the reduction process. The shift of the band from 1635 to 1637  $\text{cm}^{-1}$  is attributed to the binding of (NH) CO group with nanoparticles. It can be concluded from the FTIR study that the carboxyl ( $\text{C}=\text{O}$ ) and amine ( $\text{N}-\text{H}$ ) groups in *Afzelia quanzensis* bark extract were mainly involved in reduction of  $\text{Ag}^+$  ions to  $\text{Ag}^0$  nanoparticles.

Stability studies

A vital aspect in colloid chemistry is how nano-scale particles are stabilized in their reaction media as smaller particles are prone to agglomeration. The stability of the AgNPs in solution was checked using UV-Vis spectroscopy by observing changes in the SPR band peak [37]. Figure 12 shows UV-Vis spectra periodically obtained over 60 days. The AgNPs produced from bark extract were observed to be very stable in solution when monitored periodically over a period of 40 days; with no evidence of flocculation or change in SPR, measured at 427 nm. However, after 50 days the surface plasmon resonance absorption band decreased and can be attributed to

constant with a value from 0.9 to 1, and  $\theta$  is the Bragg angle. The average crystalline size was 19.8 nm. The obtained average crystalline size coupled with the presence of structural peaks in XRD patterns clearly illustrated that the AgNPs synthesized were nanocrystalline in nature.

FTIR analysis

The FTIR spectra of *Afzelia quanzensis* extract and synthesized AgNPs were examined (Fig. 11). The strong band at 3455  $\text{cm}^{-1}$  on the *Afzelia quanzensis* extract is characteristic of N-H and O-H stretching vibrations [35]. The characteristic absorption band at 2933  $\text{cm}^{-1}$  is due to alkyl chains. The FTIR spectra also show bands at 1637 and 1445  $\text{cm}^{-1}$  identified as amide I and amide II which arise due to carbonyl ( $\text{C}=\text{O}$ ) and amine ( $-\text{NH}$ ) stretching vibrations in the amide linkages of the proteins, respectively. The peaks at 1264 and 1060  $\text{cm}^{-1}$  may be due to a carboxylate group ( $\text{COO}^-$ ) and phosphate group, respectively. After reduction of  $\text{AgNO}_3$ , the band characteristic of N-H and O-H stretching vibrations shifted to 3424  $\text{cm}^{-1}$

Fig. 12 Stability studies

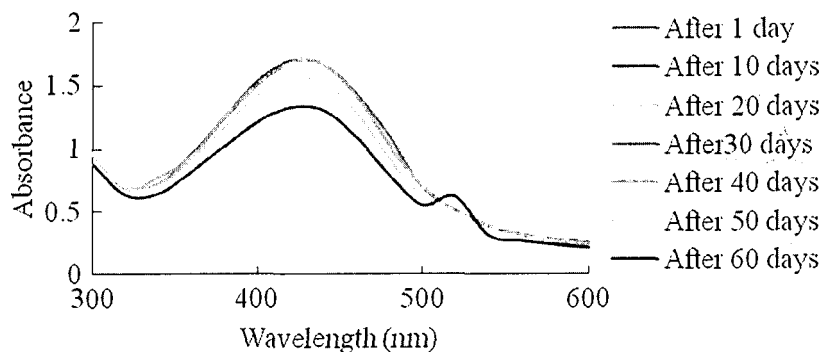
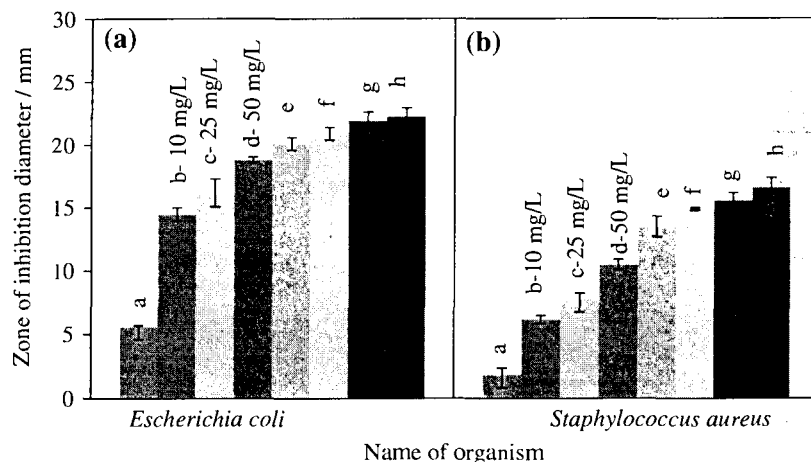


**Fig. 13** Graphical representation of inhibition zones by plant extract (a), 10 mg/L synthesized AgNPs (b), 25 mg/L synthesized AgNPs (c), 50 mg/L synthesized AgNPs (d), erythromycin (e), erythromycin plus 10 mg/L synthesized AgNPs (f), erythromycin plus 25 mg/L synthesized AgNPs (g), erythromycin plus 50 mg/L synthesized AgNPs (h), for **a** *Escherichia coli*, **b** *Staphylococcus aureus* (error bar  $\pm$ SD and  $n = 3$ )



destabilization of AgNPs in solution due to aggregation. Between 50 and 60 days secondary peaks appear at longer wavelength which is a sign of destabilization.

### Evaluation of antibacterial activity of synthesized silver nanoparticles

The antimicrobial activity of bark extract (a), synthesized AgNPs of different concentrations (b–d), the antibiotic (erythromycin) (e) and antibiotic plus different concentrations of synthesized AgNPs (f–h) were evaluated by diffusion method. The bacterial cultures used were Gram-positive bacteria, i.e. *Staphylococcus aureus* and Gram-negative bacteria, i.e. *Escherichia coli*. The increase in zone of inhibition of silver nanoparticles at different concentrations (10, 25, 50 mg/L) compared with antibiotic for both bacterial cultures (Fig. 13a, b) demonstrated the lesser antibacterial potential of silver nanoparticles with that of antibiotics. The zone of inhibition also increased with AgNPs concentration in both cultures. The bark extract exhibits the highest activity against *E. coli* than *S. aureus*. The obtained results support, at least in part, the use of this plant as traditional medicine against Gram-negative bacteria due to the presence of phytochemicals. Furthermore,

the phytosynthesized silver nanoparticles were found to be more effective against *Escherichia coli* as compared to that of *Staphylococcus aureus*. From Fig. 13a, b, it can be confirmed that combining the antibiotics with AgNPs resulted in a greater bactericidal effect on test pathogens than either of the antibacterial agents used alone. Inhibition of *Escherichia coli* might have been facilitated by silver's high affinity for phosphorus and sulphur which are part of the cell membranes of Gram-negative bacteria [38]. The sulphur and phosphorus reacts with AgNPs causing dysfunction of enzymes on bacteria cell wall and also it disturbs DNA's moieties process thereby denying replication [39]. On the other hand, the cell wall of Gram-positive bacteria is much more rigid due to the presence of a thick peptidoglycan layer, which is superficial to the cell membrane hence a difference in activity observed.

### Conclusion

The silver nanoparticles were green synthesized using bark extract of *Azelia quanzensis*. The method represents an example of clean, nontoxic and eco-friendly method for obtaining silver nanoparticles. Colour changes occur due to



429 surface plasmon resonance during the reaction with *Azela*  
 430 *quanzensis* bark extract resulting in the formation of silver  
 431 nanoparticles, which was confirmed by XRD, FTIR, UV–  
 432 Vis spectroscopy, and EDAX. The silver nanoparticles  
 433 were found to be stable in water for 40 days. The zone of  
 434 inhibition test showed that the synthesized nanoparticles  
 435 have some antibacterial activity. Further studies will be  
 436 conducted to isolate and quantify the different phyto-  
 437 chemical components and to study their pharmacological  
 438 properties after synthesizing the silver nanoparticles from  
 439 the specific phytochemicals.

441 **Compliance with ethical standards**

442 **Conflict of interest** The authors have no conflict of interest.

443 **Open Access** This article is distributed under the terms of the  
 444 Creative Commons Attribution 4.0 International License ([http://crea-](http://creativecommons.org/licenses/by/4.0/)  
 445 [tivecommons.org/licenses/by/4.0/](http://creativecommons.org/licenses/by/4.0/)), which permits unrestricted use,  
 446 distribution, and reproduction in any medium, provided you give  
 447 appropriate credit to the original author(s) and the source, provide a  
 448 link to the Creative Commons license, and indicate if changes were  
 449 made.

## 450 References

- 451 1. Kathiresan K, Manivannan S, Nabeel MA, Dhivya B (2009)  
 452 Studies on silver nanoparticles synthesized by a marine fungus,  
 453 *Penicillium fellutanum* isolated from coastal mangrove sediment.  
 454 *Colloids Surf* 71:133–137
- 455 2. Sridhara V, Pratima K, Krishnamurthy G, Sreekanth B (2013)  
 456 Vegetable assisted synthesis of silver nanoparticles and its  
 457 antibacterial activity against two human pathogens. *Asian J*  
 458 *Pharm Clin Res* 6:53–57
- 459 3. Awwad AM, Salem NM, Abdeen AO (2013) Green synthesis of  
 460 silver nanoparticles using carob leaf extract and its antibacterial  
 461 activity. *Intern J Indust Chem* 4:29–35
- 462 4. Peterson MSM, Bouwman J, Chen Deutsch AM (2007) Inorganic  
 463 metallodielectric materials fabricated using two single-step  
 464 methods based on the Tollen's process. *J Colloid Interface Sci*  
 465 306:41–49
- 466 5. Shao K, Yao J (2006) Preparation of silver nanoparticles via a  
 467 non-template method. *Mater Lett* 60:3826–3829
- 468 6. Tsuji T, Iryo K, Watanabe N, Tsuji M (2002) Preparation of  
 469 silver nanoparticles by laser ablation in solution: influence of  
 470 laser wavelength on particle size. *Appl Surf Sci* 202:80–85
- 471 7. Nagaraz B, Krishnamurthy NB, Liny P, Divya TK, Dinesh R  
 472 (2011) Biosynthesis of gold nanoparticles of *Ixora coccinea*  
 473 flower extract and their antimicrobial activities. *Int J Pharma Bio*  
 474 *Sci* 2:557–565
- 475 8. Bar H, Bhui DK, Sahoo GP, Sarkar P, De SP, Misra A (2009)  
 476 Green synthesis of silver nanoparticles using latex of *Jatropha*  
 477 *curcas*. *Colloids Surf* 339:134–139
- 478 9. Bar H, Bhui DK, Sahoo GP, Sarkar P, Pyne S, Misra A (2009)  
 479 Green synthesis of silver nanoparticles using seed extract of *Jat-*  
 480 *tropa curcas*. *Colloids Surf A* 348:212–216
- 481 10. Das VL, Thomas R, Varghese RT, Soniya EV, Mathew J, Rad-  
 482 hakrishnan EK (2014) Extracellular synthesis of silver nanopar-  
 483 ticles by the *Bacillus* strain CS 11 isolated from industrialized  
 484 area3. *Biotech* 4(2):121–126

11. Ghorbani HR (2013) Biosynthesis of silver nanoparticles using  
*Salmonella typhirium*. *J Nanostruct Chem* 3(29):1–4
12. Swarup R, Kumar DT (2014) Biosynthesis of silver nanoparticles  
 by *Aspergillus foetidus*: optimization of physicochemical  
 parameters. *Nanosci Nanotechnol Lett* 6(3):181
13. Prasad K, Anal KJ, Kulkarni AR (2007) Lactobacillus assisted  
 synthesis of titanium nanoparticles. *Nanoscale Res Lett* 2:  
 248–250
14. Jha AK, Kamallesh P, Prasad K (2009) A green low-cost  
 biosynthesis of Sb<sub>2</sub>O<sub>3</sub> nanoparticles. *Biochem Eng J* 43:303–306
15. Hebbalalu D, Lalley J, Nadagouda MN, Varma RS (2013)  
 Greener techniques for the synthesis of silver nanoparticles using  
 plant extracts, enzymes, bacteria, biodegradable polymers, and  
 microwaves. *ACS Sustain Chem Eng* 1(7):703–712
16. Prathap M, Alagesan A, Ranjitha Kumari BD (2014) Anti-bac-  
 terial activities of silver nanoparticles synthesized from plant leaf  
 extract of *Abutilon indicum* (L.) Sweet. *J Nanostruct Chem* 4:106
17. Lee SH, Salunke BK, Kim BS (2014) Sucrose density gradient  
 centrifugation separation of gold and silver nanoparticles syn-  
 thesized using *Magnolia kobus* plant leaf extracts. *Biotechnol*  
*Bioprocess Eng* 19:169–174
18. Murugan K, Senthilkumar B, Senbagam D, Al-Sohaibani S  
 (2014) Biosynthesis of silver nanoparticles using *Acacia leu-*  
*cophloea* extract and their antibacterial activity. *Int J Nanomed*  
 9:2431–2438
19. Maria BS, Devadiga A, Kodialbail VS, Saidutta MB (2015)  
 Synthesis of silver nanoparticles using medicinal *Zizyphus*  
*xylopyrus* bark extract. *Appl Nanosci*:755–762
20. Chandran SP, Chaudhary M, Pasricha R, Ahmad A, Sastry M  
 (2006) Synthesis of gold nanotriangles and silver nanoparticles  
 using *aloevera* plant extract. *Biotechnol Progress* 22:577–583
21. Sharma NC, Sahi SV, Nath S, Parsons JG, Gardea-Torresdey JL,  
 Pal T (2007) Synthesis of plant-mediated gold nanoparticles and  
 catalytic role of biomatrix embedded nanomaterials. *Environ Sci*  
*Technol* 41:5137–5142
22. Sathishkumar M, Sneha K, Won SW, Cho CW, Kim S, Yun YS  
 (2009) *Cinnamon zeylanicum* bark extract and powder mediated  
 green synthesis of nano-crystalline silver particles and its bacte-  
 ricidal activity. *Colloids Surf B* 73:332–338
23. Sathishkumar M, Sneha K, Yun YS (2010) Immobilization of  
 silver nanoparticles synthesized using curcuma longa tuber  
 powder and extract on cotton cloth for bactericidal activity.  
*Bioresour Technol* 101:7958–7965
24. Bhati-Kushwaha H, Malik CP (2014) Biosynthesis of silver  
 nanoparticles using fresh extracts of *Tridax procumbens* Linn.  
*Indian J Exp Biol* 52:359–368
25. Ahmad N, Sharma S, Alam MK, Singh VN, Shamsi SF, Mehta  
 BR, Fatma A (2010) Rapid synthesis of silver nanoparticles using  
 dried medicinal plant of basil. *Colloids Surf B* 81:81–86
26. Biegel HM (1977) Check-list of ornamental plants used in  
 Rhodesian parks and gardens. *Rhod Agric J Res Rep* 3:19–20
27. Link S, El-Sayed MA (1999) Spectral properties and relaxation  
 dynamics of surface plasmon electronic oscillations in gold and  
 silver nanodots and nanorods. *J Phys Chem B* 103:8410–8426
28. Ghadimi A, Saidur R, Metselaar HSC (2011) A review of  
 nanofluid stability properties and characterization in stationary  
 conditions. *Int J Heat Mass Transf* 54:4051–4068
29. Konishi Y, Tsukiyama TTT, Saitoh N, Nomura T, Nagamine S  
 (2007) Microbial deposition of gold nanoparticles by the metal-re-  
 ducing bacterium *Shewanella algae*. *Electrochim Acta* 53:186–192
30. Sanghi R, Verma P (2009) Biomimetic synthesis and character-  
 ization of protein capped silver nanoparticles. *Bioresour Technol*  
 100:501–504
31. Irvani S, Zolfaghari B (2013) Green synthesis of silver  
 nanoparticles using *pinus bark* extract. *Biomed Res Int* 2013:1–5

- 550 32. Gardea-Torresdey JL, Tiemann KJ, Gamez G, Dokken K, 566  
 551 Tehuacanero S, José-Yacamán M (1999) Gold nanoparticles 567  
 552 obtained by bio-precipitation from gold (III) solutions. 568  
 553 J Nanopart Res 1:397–404 569  
 554 33. Birla SS, Gaikwad SC, Gade AK, Rai MK (2013) Sci World J. 570  
 555 doi: 10.1155/2013/796018 571  
 556 34. Armendariz V, Herrera I, Peralta-Videa JR (2004) Size controlled 572  
 557 gold nanoparticle formation by *Avena sativa* biomass: use of 573  
 558 plants in nanobiotechnology. J Nanopart Res 6:377–382 574  
 559 35. Das SK, Khan MMR, Guha AK, Das AR, Mandal AB (2012) 575  
 560 Silver-nano biohybride material: synthesis, characterization and 576  
 561 application in water purification. Bioresour Technol 124:495–499 577  
 562 36. Krishnaraj C, Jagan EG, Rajasekar S, Selvakumar P, Kalaichel-  
 563 van PT, Mohan N (2010) Synthesis of silver nanoparticles using  
 564 *Acalypha indica* leaf extracts and its antibacterial activity against  
 565 water borne pathogens. Colloids Surf B 76:50–56
37. Lee DK, Tho NTM, Minhan TN, Tri MD, Sreekanth TVM, Lee JS, Nagajyothi PC (2013) Green synthesis of silver nanoparticles using *Nelumbo nucifera* seed extract and its antimicrobial activity. Acta Chim Slov 60:673–678
38. Hari N, Thomas TK, Nair AJ (2014) Comparative study on the synergistic action of differentially synthesized silver nanoparticles with  $\beta$ -Cephem antibiotics and chloramphenicol. J Nanosci 2014:1–8
39. Shetty P, Supraja N, Garud M, Prasad TNVKV (2014) Synthesis, characterization and antimicrobial activity of *Alstonia scholaris* bark-extract-mediated silver nanoparticles. J Nanostruct Chem 4(4):161–170